

# Global stability of SEIM tuberculosis model with two infection phases and medication effects

Jovian Dian Pratama, Anindita Henindya Permatasari

Department of Mathematics, Faculty of Science and Mathematics, Diponegoro University, Semarang, Indonesia

## Article Info

### Article history:

Received Sep 15, 2024

Revised Dec 16, 2024

Accepted Mar 6, 2025

### Keywords:

Basic reproduction number

Global stability analysis

SEIM model

Transmission model

Tuberculosis

## ABSTRACT

Tuberculosis (TB), caused by *mycobacterium tuberculosis* (MTB), remains a significant global health issue, leading to high morbidity and mortality rates despite being a preventable and curable disease. The dynamics of TB transmission and the effects of treatment are critical to improving disease management. This study aims to analyze the global stability of a susceptible, exposed, infected, medicated (SEIM) model for TB transmission, incorporating the effects of medication and infection phases on disease progression. A deterministic SEIM model is proposed, dividing the population into four compartments: susceptible, exposed, infected, and medicated. The model accounts for treatment effects, including non-permanent immunity and the potential dormancy of MTB. Stability analysis was conducted using Lyapunov functions to evaluate equilibrium points, and the basic reproduction number ( $\mathcal{R}_0$ ) was derived to determine disease dynamics. The analysis reveals that when  $\mathcal{R}_0 < 1$ , the system is globally asymptotically stable at the non-endemic equilibrium, indicating disease eradication. Conversely, when  $\mathcal{R}_0 > 1$ , the system converges to the endemic equilibrium, signifying sustained transmission within the population. These findings highlight the critical role of treatment and infection dynamics in controlling TB spread. The SEIM model provides a comprehensive framework for understanding TB transmission dynamics and emphasizes the importance of reducing ( $\mathcal{R}_0$ ) through effective public health interventions. Further research is recommended to validate the model with empirical data and explore its applicability in different epidemiological settings.

This is an open access article under the [CC BY-SA](#) license.



## Corresponding Author:

Anindita Henindya Permatasari

Department of Mathematics, Faculty of Science and Mathematics, Diponegoro University

Prof. Jacob Rais Street, Tembalang, Semarang 50275, Central Java, Indonesia

Email: aninditahenindya@lecturer.undip.ac.id

## 1. INTRODUCTION

Tuberculosis (TB), caused by *Mycobacterium tuberculosis* (MTB), remains one of the most pressing global health concerns. This infectious disease predominantly affects the lungs (*pulmonary tuberculosis*) but can spread to other body parts (*extrapulmonary tuberculosis*), presenting a significant public health challenge. MTB thrives in tissues with high blood and oxygen concentrations, and its slow-growing nature complicates diagnosis and treatment [1]. TB exists in two distinct phases: latent and active. Latent TB infection, characterized by the absence of microbiological, radiological, and clinical symptoms, poses no immediate threat of transmission [2], [3]. However, without appropriate treatment, 5-15% of latent cases may progress to active TB, which is highly infectious and associated with symptoms such as prolonged cough, fever, weight loss, and night sweats [4]-[6].

Despite advancements in TB management, the disease claimed approximately 1.5 million lives in 2022, reflecting a persistent burden on global health systems [7], [8]. While TB is curable with early diagnosis and comprehensive treatment, challenges remain, particularly in eradicating latent TB and managing active infections. Treatment regimens for active TB, including a combination of drugs like isoniazid, rifampin, ethambutol, and pyrazinamide, are effective but carry risks such as drug toxicity [9]-[14]. These side effects, including nausea, vision impairment, and severe complications at high doses, highlight the need for improved therapeutic strategies [15], [16].

The dynamics of TB transmission, particularly the transition between latent and active phases, remain complex and underexplored. Existing mathematical models often overlook critical factors such as varying infection phases, the effects of treatment, and the risk of drug toxicity. This gap in understanding limits the development of effective public health interventions.

This paper introduces a deterministic susceptible, exposed, infected, medicated (SEIM) model to analyze TB transmission dynamics. Unlike previous studies, this model incorporates two phases of infectivity (latent and active TB), accounts for both slow and rapid TB progression, and evaluates the impact of effective treatment on disease dynamics. The model also considers potential outcomes of medication, including MTB eradication, dormancy induction, and adverse drug reactions. Using Lyapunov functions, the study investigates the global stability of endemic and non-endemic equilibrium points, providing new insights into TB control strategies. By addressing these dynamics, the study offers a novel framework for understanding and mitigating TB transmission [17]-[19].

## 2. METHOD

### 2.1. Model formulation

This study develops a deterministic mathematical model to analyze tuberculosis (TB) dynamics by considering four population compartments: susceptible (S), exposed (E), infected (I), and medicated (M). The primary objective is to assess the stability of equilibrium points and evaluate the influence of key parameters on TB transmission. The mathematical model is represented by a system of differential equations that describe the changes in each population compartment as:

- Differential equations:

$$\begin{aligned}\frac{dS}{dt} &= \lambda - \beta S \frac{I}{N} - \mu S + (1 - q)\theta \\ \frac{dE}{dt} &= c\beta S \frac{I}{N} + q\theta M - (\mu + \alpha)E \\ \frac{dI}{dt} &= (1 - c)\beta S \frac{I}{N} + \alpha E - (\mu + \eta + \delta)I \\ \frac{dM}{dt} &= \eta I - (\mu + \theta + \gamma)M\end{aligned}$$

Here,  $N = S + E + I + M$  represents the total population size.

- Variables and parameters:

$S$  = Number of susceptible individuals.

$E$  = Number of exposed individuals.

$I$  = Number of infected individuals.

$M$  = Number of individuals receiving medication.

$\beta$  = Contact rate of infection.

$\lambda$  = Recruitment rate of new individuals into the susceptible compartment.

$\mu$  = Natural death rate.

$\alpha$  = Rate of progression to active TB from the exposed state.

$\eta$  = Medication rate.

$\delta$  = Death rate due to TB.

$\theta$  = Transition rate from medication to susceptible or exposed states.

$\gamma$  = Death rate due to complications from medication.

$q$  = Proportion of patients who enter a dormant state.

### 2.2. Analysis technique

To analyze the stability of equilibrium points, we use Lyapunov function techniques. The analysis is conducted for two primary equilibrium points:

- Non-endemic equilibrium point: Achieved when  $\mathcal{R}_0 < 1$ , indicating the disease-free state.
- Endemic equilibrium point: Achieved when  $\mathcal{R}_0 > 1$ , signifying the persistence of TB within the population.

Lyapunov function techniques are employed to prove the global stability of these equilibrium points, determining whether the solutions converge to these points over time. The basic reproduction number  $\mathfrak{R}_0$  is computed to evaluate the potential for TB spread within the population.  $\mathfrak{R}_0$  is calculated using the next-generation matrix approach:

$$\mathfrak{R}_0 = \frac{\beta\lambda(\mu+\theta+\gamma)((1-c)(\mu+\alpha)+c\alpha)}{\mu[(\mu+\alpha)(\mu+\theta+\gamma)(\mu+\eta+\delta)-\alpha q\theta\eta]}$$

An  $\mathfrak{R}_0$  value less than one indicates that the disease will decline, while an  $\mathfrak{R}_0$  value greater than one suggests the potential for endemicity.

### 2.3. Numerical simulations

Numerical simulations are performed to evaluate the impact of key parameters on TB transmission. The model is implemented using mathematical software to simulate real-world scenarios. Numerical simulations are performed to evaluate the influence of model parameters on TB dynamics. The simulations are implemented using mathematical software based on parameter values derived from relevant epidemiological studies. Key parameters, such as infection rates, contact rates, and medication rates, are taken from the literature to ensure realism and reliability in the simulations. A sensitivity analysis is conducted to determine how variations in model parameters, such as  $\beta$  (contact rate) and  $\eta$  (medication rate), affect  $\mathfrak{R}_0$  and TB transmission. This analysis helps identify the most critical factors influencing disease control.

### 2.4. Model validation, implications, and recommendations

Model validation is carried out by comparing simulation results with actual epidemiological data and previous studies. This ensures that the developed model accurately reflects TB dynamics. The results from this model provide insights into effective TB control strategies. Based on the analysis, it is recommended that public health policies focus on reducing the frequency of contact between vulnerable and infected individuals and improving medication adherence.

The model results offer valuable insights for TB control strategies. Effective interventions include:

- Reducing contact rates between vulnerable and infected individuals.
- Enhancing medication adherence to limit TB progression and transmission.

Public health policies should incorporate these findings to strengthen TB eradication efforts.

## 3. RESULTS AND DISCUSSION

The proposed SEIM model offers unique insights into tuberculosis (TB) dynamics by focusing on the role of medication and its side effects. To contextualize these findings, the results are compared with similar studies:

### a. SEIR models with vital dynamics

Studies using SEIR frameworks highlight the role of latency in delaying the spread of TB. For instance, research by Side *et al.* [20] emphasizes the equilibrium states for  $\mathfrak{R}_0 < 1$  and  $\mathfrak{R}_0 > 1$ , but lacks focus on treatment effects, a key feature in our model [21]. Our SEIM model complements these findings by integrating drug-induced dormancy and transitions between compartments, offering a more comprehensive analysis of treatment impact.

### b. Age-structured models

Research on age-structured TB models explores different transmission rates for children and adults, offering detailed stratifications of the population. However, these models generally overlook the complexities of treatment pathways, such as toxicity or incomplete recovery. By contrast, our results demonstrate how medication influences TB dynamics, providing actionable insights into therapy optimization [22], [23].

### c. Vaccination dynamics

Vaccination models, such as those presented by Aldila *et al.* [24], primarily focus on reducing the basic reproduction number ( $\mathfrak{R}_0$ ) through immunization campaigns. While effective for prevention, these models do not evaluate treatment outcomes. Our SEIM model addresses this gap by quantifying medication effects and their potential to reduce  $\mathfrak{R}_0$  through improved adherence and minimizing toxicity [25].

From a public health perspective, the results emphasize three key implications for TB control. First, reducing medication toxicity rates ( $\gamma$ ) and improving treatment adherence ( $\eta$ ) can significantly lower  $\mathfrak{R}_0$ , highlighting the necessity for safer and more effective drug regimens. Second, the inclusion of direct transitions from susceptible to infected compartments ( $1 - c$ ) suggests the need for targeted interventions to prevent rapid disease progression among high-risk populations. Finally, the study underscores the importance of combining preventive measures, such as vaccination, with robust treatment strategies to ensure comprehensive TB control.

To translate these findings into actionable policies, investments in safer medications are crucial to minimize toxicity-related mortality. Additionally, strengthening healthcare systems to enhance treatment adherence and implementing multifaceted prevention and treatment strategies are vital for achieving sustained reductions in TB prevalence. The SEIM model thus bridges significant gaps in TB modeling research, providing actionable insights that align with public health priorities.

### 3.1. Model formulation

Three compartments comprise the transmission model: susceptible individuals ( $S$ ), exposed individuals (those infected with  $M.$  tuberculosis but not clinically ill and hence noninfectious) ( $E$ ), infected individuals (those with active TB) ( $I$ ), and medicated individuals (those receiving medication) ( $M$ ).  $N(t) = S(t) + E(t) + I(t) + M(t)$  is the total number of people at time  $t$ .

Individuals in the susceptible class ( $S$ ) have a contact rate with infected individuals of  $\beta I/N$ , where  $0 < \beta \leq 1$  is the probability of a susceptible individual being infected by an infected individual. The recruitment rate in the susceptible subpopulation is denoted by  $\lambda$ . Susceptible individuals can be exposed to MTB and move to subpopulation  $E$  with a probability of  $c$ , where  $0 < c \leq 1$ . Susceptible individuals infected with the MTB virus can become infected without first becoming an exposed individual with a probability of  $(1 - c)$ . Exposed individuals can develop active TB at the rate  $\alpha > 0$ . Infected individuals undergo medication at the level  $\eta > 0$  and move to the subpopulation  $M(t)$ . Infected individuals have a risk of death from TB disease at the rate  $\delta > 0$ , while the natural death rate in each subpopulation is  $\mu > 0$ . It is assumed that administering drugs to individuals infected with TB gives three reactions. The first reaction is that the MTB in the body disappears so that the individual will return to being a susceptible individual with a rate  $(1 - q)\theta$ . The second reaction is to make the active TB virus inactive (dormancy) so that the individual will return to being an exposed individual with a rate  $q\theta$ . The last, administering drugs can cause someone to die due to poisoning, liver damage, or overdose with a rate  $\gamma > 0$ .

The transmission model can be written as the system of nonlinear differential equations, as in (1).

$$\begin{aligned}\frac{dS}{dt} &= \lambda - \beta S \frac{I}{N} - \mu S + (1 - q)\theta \\ \frac{dE}{dt} &= c\beta S \frac{I}{N} + q\theta M - (\mu + \alpha)E \\ \frac{dI}{dt} &= (1 - c)\beta S \frac{I}{N} + \alpha E - (\mu + \eta + \delta)I \\ \frac{dM}{dt} &= \eta I - (\mu + \theta + \gamma)M\end{aligned}\quad (1)$$

Figure 1 displays the (1) transfer diagram. The fractions of the class susceptible, exposed, infected, and medicated (drugged) in the population are represented, respectively, by the variables  $v = \frac{S}{N}$ ,  $w = \frac{E}{N}$ ,  $x = \frac{I}{N}$ , and  $y = \frac{M}{N}$ . Verifying that  $v, w, x$ , and  $y$  fulfill the differential equation system is simple,

$$\begin{aligned}\frac{dv}{dt} &= \lambda - \beta vx - \mu v + (1 - q)\theta y \\ \frac{dw}{dt} &= c\beta vx + q\theta y - (\mu + \alpha)w \\ \frac{dx}{dt} &= (1 - c)\beta vx + \alpha w - (\mu + \eta + \delta)x \\ \frac{dy}{dt} &= \eta x - (\mu + \theta + \gamma)y\end{aligned}\quad (2)$$

subject to the restriction  $v + w + x + y = 1$ .

Given that (2) depicts the human population, it is imperative to reveal that every state variable is nonnegative. The following subsection provides an explanation of these fundamental characteristics.

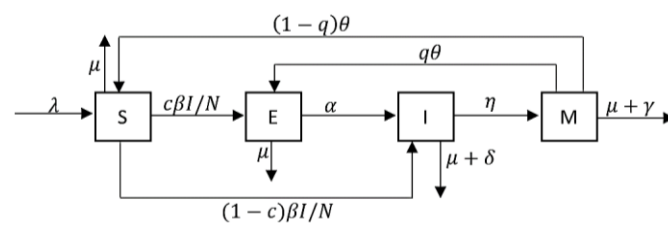


Figure 1. Transfer diagram for dynamic (1)

### 3.2. Positivity of solutions and invariant region

#### 3.2.1. Positivity of solutions

To demonstrate the epidemiological significance of the TB model, we shall demonstrate that every variable in (2) is non-negative for all times  $t > 0$ . This leads us to the following lemma.

Lemma 1. The solutions  $v(t)$ ,  $w(t)$ ,  $x(t)$ , and  $y(t)$  of the (2) are positive for all  $t > 0$  if  $v(0) \geq 0$ ,  $w(0) \geq 0$ ,  $x(0) \geq 0$ , and  $y(0) \geq 0$ . Proof: the first equation of (2) states that if  $v(0)$ ,  $w(0)$ ,  $x(0)$ , and  $y(0)$  are all zero, then  $\frac{dv(t)}{dt} = \lambda - \beta v(t)x(t) - \mu v(t) + (1 - q)\theta y(t)$ .

Rewriting it would look like this (3).

$$\begin{aligned} \frac{dv(t)}{dt} + \beta v(t)x(t) + \mu v(t) &= \lambda + (1 - q)\theta y(t) \\ \frac{dv(t)}{dt} + v(t)(\beta x(t) + \mu) \exp\left(\mu t + \int_0^t \beta x(u) du\right) &= (\lambda + (1 - q)\theta y(t)) \exp\left(\mu t + \int_0^t \beta x(u) du\right) \\ \frac{d}{dt}\left(v(t) \exp\left(\mu t + \int_0^t \beta x(u) du\right)\right) &= (\lambda + (1 - q)\theta y(t)) \exp\left(\mu t + \int_0^t \beta x(u) du\right) \end{aligned} \quad (3)$$

Integrating both sides, we get (4).

$$v(t) \exp\left(\mu t + \int_0^t \beta x(u) du\right) - v(0) = \int_0^t (\lambda + (1 - q)\theta y(a)) \exp\left(\mu a + \int_0^a \beta x(u) du\right) da \quad (4)$$

Therefore,  $v(t)$  answer is (5).

$$\begin{aligned} v(t) &= v(0) \exp\left(-\mu t - \int_0^t \beta x(u) du\right) \\ &+ \exp\left(-\mu t - \int_0^t \beta x(u) du\right) \int_0^t (\lambda + (1 - q)\theta y(a)) \exp\left(\mu a + \int_0^a \beta x(u) du\right) da > 0, \forall t > 0. \end{aligned} \quad (5)$$

Likewise, we may demonstrate that  $w(t)$ ,  $x(t)$ , and  $y(t) > 0$ . Thus, for any  $t > 0$ , the (2) solutions  $v(t)$ ,  $w(t)$ ,  $x(t)$ , and  $y(t)$  are positive. So, we have (6).

$$\frac{dv(t)}{dt} = \lambda - \beta v(t)x(t) - \mu v(t) + (1 - q)\theta y(t). \quad (6)$$

Rewriting it (6) would look like this:  $\frac{dv(t)}{dt} + \beta v(t)x(t) + \mu v(t) = \lambda + (1 - q)\theta y(t)$ .

#### 3.2.2. Invariant region

The biological importance of our (2) can be determined by analyzing it within a suitable and practical region  $\Omega$  and demonstrating that the parameters and variables are non-negative for all times  $t \geq 0$ .

Lemma 2. In (2) positively invariantly defines the feasible region  $\Omega$  as (7).

$$\Omega = \left\{ (v(t), w(t), x(t), y(t)) \in \mathbb{R}_+^4 : 0 \leq v(t) + w(t) + x(t) + y(t) \leq \frac{\lambda}{\mu} \right\} \quad (7)$$

With starting condition  $v(0) \geq 0$ ,  $w(0) \geq 0$ ,  $x(0) \geq 0$ ,  $y(0) \geq 0$ .

Proof. In (2) are added to yield (8).

$$\frac{dN(t)}{dt} = \frac{dv(t)}{dt} + \frac{dw(t)}{dt} + \frac{dx(t)}{dt} + \frac{dy(t)}{dt} = \lambda - \mu N(t) - \delta x(t) - \gamma y(t) < \lambda - \mu N(t) \quad (8)$$

In (2) is examined to determine the fundamental reproduction ratio and investigate the stability of both endemic and non-endemic equilibrium.  $0 \leq N(t) \leq \frac{\lambda}{\mu} + N(0)e^{-\mu t}$ , where  $N(0)$  represents the starting values of the entire population, follows. Thus, as  $t \rightarrow \infty$ ,  $0 \leq N(t) \leq \frac{\lambda}{\mu}$ . Thus, for (2), the region (7) is a positively invariant set. The dynamics of equations (2) on the region  $\Omega$  will be examined.

### 3.3. Basic reproduction ratio

We use the next-generation matrix to derive the basic reproduction ratio,  $\mathfrak{R}_0$ , to analyze the stability of non-endemic equilibrium [26], [27].  $UEP_0 = \left(\frac{\lambda}{\mu}, 0, 0, 0\right)$  is the non-endemic equilibrium point of the (2). According to [28], [29], the basic reproduction ratio  $\mathfrak{R}_0$  for (1) through (8) is as (9).

$$\mathfrak{R}_0 = \frac{\beta \lambda (\mu + \theta + \gamma) ((1 - c)(\mu + \alpha) + c\alpha)}{\mu [(\mu + \alpha)(\mu + \theta + \gamma)(\mu + \eta + \delta) - \alpha q \theta \eta]} \quad (9)$$

The following subsection presents the local stability of equilibrium.

### 3.4. Global stability of non-endemic equilibrium

We employ Lyapunov stability to demonstrate the global strength of the non-endemic equilibrium point  $UEP_0$ . Theorem 1 can be utilized to illustrate the global stability of  $UEP_0$ . Theorem 1 [30], [31] states that when  $\mathfrak{R}_0 < 1$  then equilibrium point  $UEP_0$  is globally asymptotically stable. Proof. Given the candidate Lyapunov function, as in (10).

$$V = A_1 w + A_2 x + A_3 y \quad (10)$$

Which was motivated by Savadogo *et al.* [32] and Aziz-Alaoui *et al.* [33], where  $A_1, A_2$ , and  $A_3$  are positive constants that will be found later.

$\dot{V} = A_1 \dot{w} + A_2 \dot{x} + A_3 \dot{y}$  is its derivative along the solutions to (2), we have (11).

$$\begin{aligned} \dot{V} &= A_1 (c\beta vx + q\theta y - (\mu + \alpha)w) + A_2 ((1 - c)\beta vx + \alpha w - (\mu + \eta + \delta)x) \\ &\quad + A_3 (\eta x - (\mu + \theta + \gamma)y). \\ \dot{V} &= (-A_1(\mu + \alpha) + A_2\alpha)w + (-A_2(\mu + \eta + \delta) + A_3\eta + A_1c\beta v + A_2(1 - c)\beta v)x \\ &\quad + (A_1q\theta - A_3(\mu + \theta + \gamma))y \end{aligned} \quad (11)$$

The coefficients of  $w$  are set to equal zero by the constants  $A_1$  and  $A_2$ . Consequently, we have (12).

$$A_1 = \alpha, A_2 = (\mu + \alpha) \quad (12)$$

In a similar vein, the constant  $A_3$  is selected so that  $y$ 's coefficients equal zero. We obtain (13).

$$A_3 = \frac{A_1 q \theta}{(\mu + \theta + \gamma)} \quad (13)$$

Since  $A_1 = \alpha$ , we have (14).

$$A_3 = \frac{\alpha q \theta}{(\mu + \theta + \gamma)} \quad (14)$$

Finally, we obtain (15) after inserting in the positive constants  $A_1, A_2$ , and  $A_3$  from (13) in (14).

$$\begin{aligned} \dot{V} &= \left[ -(\mu + \alpha)(\mu + \eta + \delta) + \frac{\alpha q \theta}{(\mu + \theta + \gamma)} \eta + \alpha c \beta v + (\mu + \alpha)(1 - c)\beta v \right] x \\ \dot{V} &= \frac{1}{(\mu + \theta + \gamma)} \left[ \beta((1 - c)\mu + \alpha)(\mu + \theta + \gamma) \right] \left[ v - \frac{1}{\mathfrak{R}_0} \right] x \end{aligned} \quad (15)$$

As  $v \leq v_0$ , we possess (16).

$$\dot{V} \leq \frac{\beta((1 - c)\mu + \alpha)(\mu + \theta + \gamma)x}{(\mu + \theta + \gamma)} \left[ 1 - \frac{1}{\mathfrak{R}_0} \right] \quad (16)$$

Moreover,  $\dot{V} = 0$  only holds for  $\mathfrak{R}_0 = 1$  or  $x = 0$ . The  $UEP_0$  is the greatest invariant set in  $\{(v, w, x, y) : \dot{V} = 0\}$ . The LaSalle's invariance principle [34]-[36] states that  $UEP_0$  is globally stable when  $\mathfrak{R}_0 < 1$ .

### 3.5. Global stability of non-endemic equilibrium

The (2) has endemic equilibrium point  $EEP^* = (v^*, w^*, x^*, y^*)$ , where (17).

$$\begin{aligned} v^* &= \frac{\lambda}{\mu \mathfrak{R}_0}, \\ w^* &= \frac{\mu(q\theta\eta(1-c) + (\mu + \theta + \gamma)(\mu + \eta + \delta)c)((\mu + \alpha)(\mu + \theta + \gamma)(\mu + \eta + \delta) - \alpha q \theta \eta)}{\beta(\mu + \theta + \gamma)(c\alpha + (1 - c)(\mu + \alpha))((\mu + \alpha)(\mu + \theta + \gamma)(\mu + \eta + \delta) - \alpha q \theta \eta - (1 - q)\theta\eta(c\alpha + (1 - c)(\mu + \alpha)))} (\mathfrak{R}_0 - 1), \\ x^* &= \frac{\mu((\mu + \alpha)(\mu + \theta + \gamma)(\mu + \eta + \delta) - \alpha q \theta \eta)}{\beta((\mu + \alpha)(\mu + \theta + \gamma)(\mu + \eta + \delta) - \alpha q \theta \eta - (1 - q)\theta\eta(c\alpha + (1 - c)(\mu + \alpha)))} (\mathfrak{R}_0 - 1), \\ y^* &= \frac{\mu\eta((\mu + \alpha)(\mu + \theta + \gamma)(\mu + \eta + \delta) - \alpha q \theta \eta)}{\beta(\mu + \theta + \gamma)((\mu + \alpha)(\mu + \theta + \gamma)(\mu + \eta + \delta) - \alpha q \theta \eta - (1 - q)\theta\eta(c\alpha + (1 - c)(\mu + \alpha)))} (\mathfrak{R}_0 - 1). \end{aligned} \quad (17)$$

Thus, the endemic equilibrium is present when  $\mathfrak{R}_0 > 1$ . Later, the global stability of  $EEP^*$  is demonstrated using Theorem 2.

Theorem 2. When  $\mathfrak{R}_0 > 1$ , the endemic equilibrium point  $EEP^*$  is globally asymptotically stable.

Proof. For the endemic equilibrium  $EEP^*$ ,  $v^*$ ,  $w^*$ ,  $x^*$ , and  $y^*$  satisfies (18).

$$\begin{aligned}\lambda - \beta v^* x^* - \mu v^* + (1 - q)\theta y^* &= 0 \\ c\beta v^* x^* + q\theta y^* - (\mu + \alpha)w^* &= 0 \\ (1 - c)\beta v^* x^* + \alpha w^* - (\mu + \eta + \delta)x^* &= 0 \\ \eta x^* - (\mu + \theta + \gamma)y^* &= 0\end{aligned}\quad (18)$$

Motivated by [30], [31], we consider the Lyapunov function as (19).

$$F = (v - v^* \ln v) + c_1(w - w^* \ln w) + c_2(x - x^* \ln x) + c_3(y - y^* \ln y) \quad (19)$$

Where the positive constants  $c_1$ ,  $c_2$ , and  $c_3$  are to be found subsequently. As we differentiate  $F$  concerning  $t$  along the (2) solutions, we obtain (20).

$$\begin{aligned}\dot{F} &= \left(1 - \frac{v^*}{v}\right) \dot{v} + c_1 \left(1 - \frac{w^*}{w}\right) \dot{w} + c_2 \left(1 - \frac{x^*}{x}\right) \dot{x} + c_3 \left(1 - \frac{y^*}{y}\right) \dot{y} \\ \dot{F} &= \left(1 - \frac{v^*}{v}\right) (\lambda - \beta vx - \mu v + (1 - q)\theta y) + c_1 \left(1 - \frac{w^*}{w}\right) (c\beta vx + q\theta y - (\mu + \alpha)w) \\ &+ c_2 \left(1 - \frac{x^*}{x}\right) ((1 - c)\beta vx + \alpha w - (\mu + \eta + \delta)x) \\ &+ c_3 \left(1 - \frac{y^*}{y}\right) (\eta x - (\mu + \theta + \gamma)y) \\ \dot{F} &= (\lambda + c_1(\mu + \alpha)w^* + c_2(\mu + \eta + \delta)x^* + c_3(\mu + \theta + \gamma)y^*) - \lambda \frac{v^*}{v} \\ &+ (-c_1(\mu + \alpha) + c_2\alpha)w + (\beta v^* + c_3\eta - c_2(\mu + \eta + \delta))x \\ &+ ((1 - q)\theta + c_1q\theta - c_3(\mu + \theta + \gamma))y \\ &+ (-\beta + c_1c\beta + c_2(1 - c)\beta)vx + \mu v^* - \mu v - \left((1 - q)\theta y^* \frac{y}{y^*} \frac{v^*}{v}\right) \\ &- \left(c_1c\beta v^* x^* \frac{v}{v^*} \frac{x}{x^*} \frac{w^*}{w} + c_1q\theta y^* \frac{y}{y^*} \frac{w^*}{w}\right) \\ &- \left(c_2(1 - c)\beta v^* \frac{v}{v^*} x^* + c_2\alpha w^* \frac{w}{w^*} \frac{x^*}{x}\right) - \left(c_3\eta x^* \frac{x}{x^*} \frac{y^*}{y}\right)\end{aligned}\quad (20)$$

By considering in (18), one has (21).

$$\begin{aligned}\lambda &= \beta v^* x^* + \mu v^* - (1 - q)\theta y^* \\ (\mu + \alpha)w^* &= c\beta v^* x^* + q\theta y^* \\ (\mu + \eta + \delta)x^* &= (1 - c)\beta v^* x^* + \alpha w^* \\ (\mu + \theta + \gamma)y^* &= \eta x^*\end{aligned}\quad (21)$$

By using first equation until forth equation of system (18), in (19) becomes (20).

$$\begin{aligned}\dot{F} &= \beta v^* x^* \left(1 - \frac{v^*}{v}\right) - (1 - q)\theta y^* \left(1 - \frac{v^*}{v}\right) + c_1c\beta v^* x^* \left(1 - \frac{v}{v^*} \frac{x}{x^*} \frac{w^*}{w}\right) \\ &+ c_1q\theta y^* \left(1 - \frac{y}{y^*} \frac{w^*}{w}\right) + c_2(1 - c)\beta v^* x^* \left(1 - \frac{v}{v^*}\right) \\ &+ c_2\alpha w^* \left(1 - \frac{w}{w^*} \frac{x^*}{x}\right) + c_3\eta x^* \left(1 - \frac{x}{x^*} \frac{y^*}{y}\right) + (-c_1(\mu + \alpha) + c_2\alpha)w \\ &+ (\beta v^* + c_3\eta - c_2(\mu + \eta + \delta))x \\ &+ ((1 - q)\theta + c_1q\theta - c_3(\mu + \theta + \gamma))y \\ &+ (-\beta + c_1c\beta + c_2(1 - c)\beta)vx + \mu v^* \left(2 - \frac{v}{v^*} - \frac{v^*}{v}\right) \\ &- \left((1 - q)\theta y^* \frac{y}{y^*} \frac{v^*}{v}\right)\end{aligned}\quad (22)$$

Let  $A = \frac{v}{v^*}$ ,  $B = \frac{w}{w^*}$ ,  $C = \frac{x}{x^*}$ ,  $D = \frac{y}{y^*}$ , then in (22) becomes (23).

$$\begin{aligned}
\dot{F} = & \mu v^* \left(2 - A - \frac{1}{A}\right) + \beta v^* x^* \left(1 - \frac{1}{A}\right) + c_1 c \beta v^* x^* \left(1 - \frac{AC}{B}\right) + c_2 (1 - c) \beta v^* x^* (1 - A) \\
& + c_1 q \theta y^* \left(1 - \frac{D}{B}\right) + c_2 \alpha w^* \left(1 - \frac{B}{C}\right) + c_3 \eta x^* \left(1 - \frac{C}{D}\right) \\
& - (1 - q) \theta y^* \left(1 - \frac{1}{A}\right) - \left((1 - q) \theta y^* \frac{D}{A}\right) + (-c_1 (\mu + \alpha) + c_2 \alpha) w \\
& + (\beta v^* + c_3 \eta - c_2 (\mu + \eta + \delta)) x \\
& + ((1 - q) \theta + c_1 q \theta - c_3 (\mu + \theta + \gamma)) y \\
& + (-\beta + c_1 c \beta + c_2 (1 - c) \beta) vx
\end{aligned} \tag{23}$$

Making the coefficients  $w, x, y, vx$  are equal to 0, so we have the relationship (24).

$$\begin{aligned}
c_1 (\mu + \alpha) &= c_2 \alpha \\
c_2 (\mu + \eta + \delta) &= \beta v^* + c_3 \eta \\
c_3 (\mu + \theta + \gamma) &= (1 - q) \theta + c_1 q \theta \\
c_1 c + c_2 (1 - c) &= 1
\end{aligned} \tag{24}$$

We obtain (25).

$$c_1 = \frac{\alpha}{(\alpha c + (1 - c)(\mu + \alpha))}, c_2 = \frac{(\mu + \alpha)}{(\alpha c + (1 - c)(\mu + \alpha))}, c_3 = \frac{(1 - q)\theta + c_1 q \theta}{(\mu + \theta + \gamma)} \tag{25}$$

Replacing the expressions of  $c_1, c_2$  and  $c_3$  in (23) then we get (26).

$$\begin{aligned}
\dot{F} = & \mu v^* \left(2 - A - \frac{1}{A}\right) + c_1 c \beta v^* x^* \left(1 - \frac{1}{A}\right) + c_2 (1 - c) \beta v^* x^* \left(1 - \frac{1}{A}\right) \\
& + c_1 c \beta v^* x^* \left(1 - \frac{AC}{B}\right) + c_2 (1 - c) \beta v^* x^* (1 - A) + c_1 q \theta y^* \left(1 - \frac{D}{B}\right) \\
& + c_2 \alpha w^* \left(1 - \frac{B}{C}\right) + c_3 \eta x^* \left(1 - \frac{C}{D}\right) - (1 - q) \theta y^* \left(1 - \frac{1}{A}\right) \\
& - \left((1 - q) \theta y^* \frac{D}{A}\right) + (-c_1 (\mu + \alpha) + c_2 \alpha) w \\
& + (\beta v^* + c_3 \eta - c_2 (\mu + \eta + \delta)) x \\
& + ((1 - q) \theta + c_1 q \theta - c_3 (\mu + \theta + \gamma)) y \\
& + (-\beta + c_1 c \beta + c_2 (1 - c) \beta) vx
\end{aligned} \tag{26}$$

Using the fact that  $c_1 c + c_2 (1 - c) = 1$ , in (26) becomes (27).

$$\begin{aligned}
\dot{F} = & \mu v^* \left(2 - A - \frac{1}{A}\right) + c_1 c \beta v^* x^* \left(2 - \frac{1}{A} - \frac{AC}{B}\right) \\
& + c_2 (1 - c) \beta v^* x^* \left(2 - A - \frac{1}{A}\right) + c_1 q \theta y^* \left(1 - \frac{D}{B}\right) + c_2 \alpha w^* \left(1 - \frac{B}{C}\right) + c_3 \eta x^* \left(1 - \frac{C}{D}\right) \\
& - (1 - q) \theta y^* \left(1 - \frac{1}{A}\right) - \left((1 - q) \theta y^* \frac{D}{A}\right) + (-c_1 (\mu + \alpha) + c_2 \alpha) w \\
& + (\beta v^* + c_3 \eta - c_2 (\mu + \eta + \delta)) x \\
& + ((1 - q) \theta + c_1 q \theta - c_3 (\mu + \theta + \gamma)) y \\
& + (-\beta + c_1 c \beta + c_2 (1 - c) \beta) vx
\end{aligned} \tag{27}$$

Multiplying the second equation of (13) by  $c_1$  and the first equation of (16) by  $w^*$  gives (28).

$$\begin{aligned}
c_1 (\mu + \alpha) w^* &= c_1 c \beta v^* x^* + c_1 q \theta y^* \\
c_1 (\mu + \alpha) w^* &= c_2 \alpha w^*
\end{aligned} \tag{28}$$

We can deduce that,

$$c_1 c \beta v^* x^* + c_1 q \theta y^* - c_2 \alpha w^* = 0 \tag{29}$$

Now, multiplying the above equation by  $F_1(u)$  where  $u = (A, B, C, D)^T$  and  $F_1(u)$  will be determined later yields (30).

$$c_1 c \beta v^* x^* F_1(u) + c_1 q \theta y^* F_1(u) - c_2 \alpha w^* F_1(u) = 0 \tag{30}$$



Next, multiplying the third equation of (21) by  $c_2$  and the second equation of (24) by  $x^*$  gives (31).

$$\begin{aligned}c_2(\mu + \eta + \delta)x^* &= c_2(1 - c)\beta v^*x^* + c_2\alpha w^* \\c_2(\mu + \eta + \delta)x^* &= \beta v^*x^* + c_3\eta x^*\end{aligned}\quad (31)$$

We can write (31) as (32).

$$c_2(1 - c)\beta v^*x^* + c_2\alpha w^* - \beta v^*x^* - c_3\eta x^* = 0 \quad (32)$$

Using the fact that  $c_1c + c_2(1 - c) = 1$ , the (32) becomes (33).

$$c_2\alpha w^* - c_1c\beta v^*x^* - c_3\eta x^* = 0 \quad (33)$$

Now, multiplying the (33) by  $F_2(u)$  where  $u = (A, B, C, D)^T$  and  $F_2(u)$  will be determined later yields (34).

$$c_2\alpha w^*F_2(u) - c_1c\beta v^*x^*F_2(u) - c_3\eta x^*F_2(u) = 0 \quad (34)$$

Next, multiplying the last equation of (21) by  $c_3$  and the third equation of (24) by  $y^*$  gives (35)

$$\begin{aligned}c_3(\mu + \theta + \gamma)y^* &= c_3\eta x^* \\c_3(\mu + \theta + \gamma)y^* &= (1 - q)\theta y^* + c_1q\theta y^*\end{aligned}\quad (35)$$

We can state (35) as (36).

$$c_3\eta x^* - (1 - q)\theta y^* - c_1q\theta y^* = 0 \quad (36)$$

Multiplying the (36) by  $F_3(u)$  where  $u = (A, B, C, D)^T$  and  $F_3(u)$  will be determined later yields (37).

$$c_3\eta x^*F_3(u) - (1 - q)\theta y^*F_3(u) - c_1q\theta y^*F_3(u) = 0 \quad (37)$$

Adding the (30), (34), and (37) into (27), we obtain (38).

$$\begin{aligned}\dot{F} &= \mu v^* \left(2 - A - \frac{1}{A}\right) + c_1c\beta v^*x^* \left(2 - \frac{1}{A} - \frac{AC}{B} - F_1(u) + F_2(u)\right) \\&+ c_2(1 - c)\beta v^*x^* \left(2 - A - \frac{1}{A}\right) + c_1q\theta y^* \left(1 - \frac{D}{B} - F_1(u) + F_3(u)\right) \\&+ c_2\alpha w^* \left(1 - \frac{B}{C} + F_1(u) - F_2(u)\right) + c_3\eta x^* \left(1 - \frac{C}{D} + F_2(u) - F_3(u)\right) \\&- (1 - q)\theta y^* \left(1 - \frac{1}{A} - F_3(u)\right) - \left((1 - q)\theta y^* \frac{D}{A}\right)\end{aligned}\quad (38)$$

The functions  $F_1(u)$ ,  $F_2(u)$ , and  $F_3(u)$  are chosen such that the coefficients of  $y^*$  and  $w^*$  are equal to zero. In this case, we have (39).

$$F_1(u) = 2 - \frac{1}{A} - \frac{D}{B}, F_2(u) = 3 - \frac{B}{C} - \frac{1}{A} - \frac{D}{B}, \text{ and } F_3(u) = 1 - \frac{1}{A} \quad (39)$$

Finally, we get (40).

$$\begin{aligned}\dot{F} &= \mu v^* \left(2 - A - \frac{1}{A}\right) + c_1c\beta v^*x^* \left(3 - \frac{1}{A} - \frac{B}{C} - \frac{AC}{B}\right) \\&+ c_2(1 - c)\beta v^*x^* \left(2 - A - \frac{1}{A}\right) + c_3\eta x^* \left(3 - \frac{C}{D} - \frac{B}{C} - \frac{D}{B}\right) \\&- \left((1 - q)\theta y^* \frac{D}{A}\right)\end{aligned}\quad (40)$$

Given that the geometrical mean equals or exceeds the arithmetical mean,  $2 - A - \frac{1}{A} \leq 0$  for  $A > 0$  and  $2 - A - \frac{1}{A} = 0$  if and only if  $A = 1$ . Then,  $3 - \frac{1}{A} - \frac{B}{C} - \frac{AC}{B} \leq 0$  for  $A, B, C > 0$  and  $3 - \frac{1}{A} - \frac{B}{C} - \frac{AC}{B} = 0$  if and only if  $A = B = C = 1$ . Also,  $3 - \frac{C}{D} - \frac{B}{C} - \frac{D}{B} \leq 0$  for  $B, C, D > 0$  and  $3 - \frac{C}{D} - \frac{B}{C} - \frac{D}{B} = 0$  if and only if  $B = C =$

$D = 1$ . Therefore, the maximum invariant set of the equations (2) on the set  $(A, B, C, D) : \dot{F} = 0$  is  $(1, 1, 1, 1)$ , and  $\dot{F} \leq 0$  for  $A, B, C, D > 0$  and  $\dot{F} = 0$  if and only if  $A = B = C = D = 1$ . According to the LaSalle Invariance Principle [34]-[36], in (2) endemic equilibrium point,  $EEP^*$ , is thus globally asymptotically stable if  $\mathfrak{R}_0 > 1$ .

### 3.6. Sensitivity analysis

Sensitivity analysis is a crucial tool in understanding the robustness of epidemiological models, especially in determining how various parameters affect the basic reproduction number ( $\mathfrak{R}_0$ ), which is a key indicator of disease transmission potential [37]. Numerous studies have demonstrated the importance of analyzing the sensitivity of model parameters in controlling infectious diseases, including tuberculosis (TB) [38], [39]. By identifying the most influential parameters, such as contact rates or treatment rates, researchers can better allocate resources and design targeted interventions.

We perform sensitivity analysis of reproduction number  $\mathfrak{R}_0$  in this section to see the effect of  $\theta$  and  $\eta$  on  $\mathfrak{R}_0$ . The reproduction number  $\mathfrak{R}_0$  is given by the following equation in (5), so that (41).

$$\mathfrak{R}_0 = \frac{\beta\lambda(\mu+\theta+\gamma)((1-c)(\mu+\alpha)+c\alpha)}{\mu[(\mu+\alpha)(\mu+\theta+\gamma)(\mu+\eta+\delta)-\alpha q\theta\eta]} \quad (41)$$

we look for the derivative with respect to  $\beta$ , we obtain (42).

$$\frac{\partial \mathfrak{R}_0}{\partial \beta} = \frac{\lambda(\mu+\theta+\gamma)((1-c)(\mu+\alpha)+c\alpha)}{\mu[(\mu+\alpha)(\mu+\theta+\gamma)(\mu+\eta+\delta)-\alpha q\theta\eta]} \quad (42)$$

When  $(\mu + \alpha)(\mu + \theta + \gamma)(\mu + \eta + \delta) > \alpha q\theta\eta$ , we have  $\frac{\partial \mathfrak{R}_0}{\partial \beta} > 0$ . It means that  $\mathfrak{R}_0$  increases when  $\beta$  increases. After that, we look for the derivative with respect to  $\eta$ , we obtain (43).

$$\frac{\partial \mathfrak{R}_0}{\partial \eta} = -\frac{\beta\lambda((1-c)(\mu+\alpha)+c\alpha)((\mu+\alpha)(\mu+\theta+\gamma)-\alpha q\theta)}{\mu((\mu+\alpha)(\mu+\theta+\gamma)(\mu+\eta+\delta)-\alpha q\theta\eta)^2} \quad (43)$$

When  $\beta\lambda((1-c)(\mu+\alpha)+c\alpha)((\mu+\alpha)(\mu+\theta+\gamma)-\alpha q\theta) > 0$ , we have  $\frac{\partial \mathfrak{R}_0}{\partial \eta} < 0$ . It means that  $\mathfrak{R}_0$  decreases when  $\eta$  increases.

Biologically, this means that infected individuals which are medicated have great negative influence on the spread of the tuberculosis. Figure 2 shows the relationship among  $\mathfrak{R}_0$ ,  $\theta$ , and  $\eta$  when we set  $\mu = 0.05, \lambda = 1, \beta = 0.03, \alpha = 0.2, c = 0.9, \gamma = 0.12, q = 0.5, \delta = 0.5, \eta = 0.09$ , and  $\theta = 0.02$ .

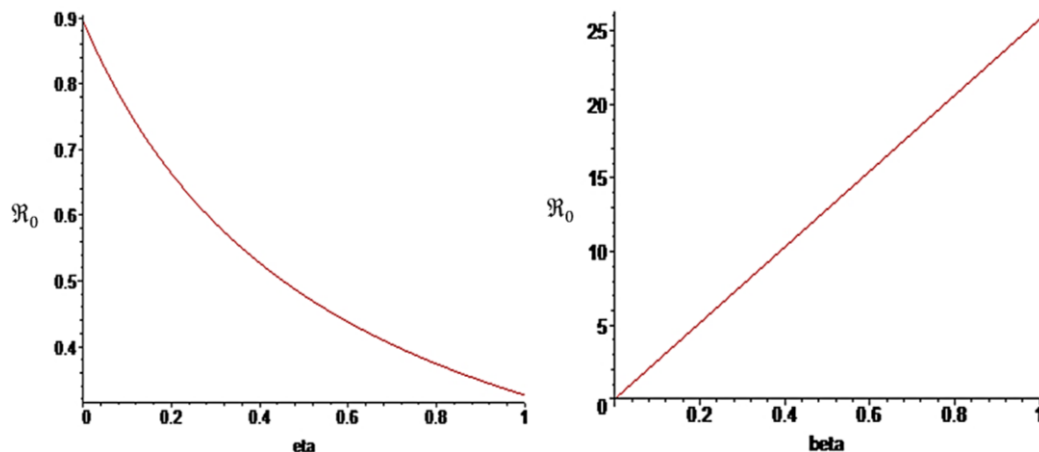
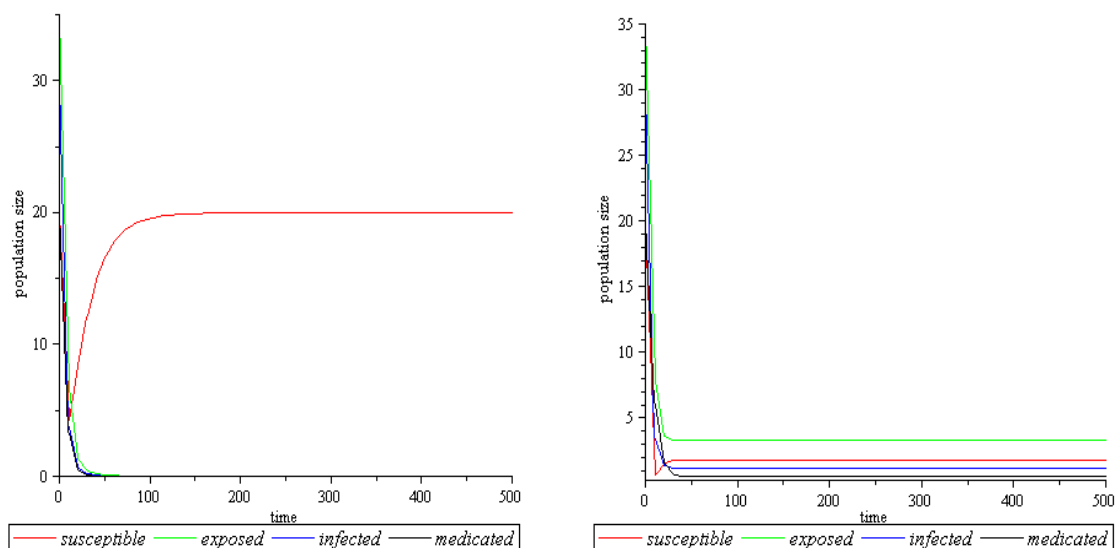
### 3.7. Numerical simulation

Numerical simulations play a critical role in validating theoretical results and providing visual insights into the dynamic behavior of infectious disease models. They help demonstrate how different parameter values affect the trajectory of the disease over time, especially in models of complex diseases such as tuberculosis (TB) [40]. Previous studies have shown the importance of simulating TB models to understand the long-term effects of interventions and the behavior of disease transmission in different population groups [41], [42]. By adjusting key parameters such as the transmission rate ( $\beta$ ) and the medication rate ( $\eta$ ), we can observe how these factors influence the stability of the disease-free and endemic equilibria.

We will give some simulations to illustrate the theoretical analysis of (2). First, we set  $\mu = 0.05, \lambda = 1, \beta = 0.03, \alpha = 0.2, c = 0.9, \gamma = 0.12, q = 0.5, \delta = 0.5, \eta = 0.09, \theta = 0.02$  and we have  $\mathfrak{R}_0 = 0.7733 < 1$ . Figure 3 presents the trajectory plot of (2) when  $\mathfrak{R}_0 < 1$ . Figure 3 illustrates how (2) trajectory map converges to the non-endemic equilibrium. In other words, as Theorem 1 illustrates, the disease eventually disappears from the population.

Second, we change the value of  $\beta$  and  $\eta$ . We choose  $\beta = 0.43, \eta = 0.01$  and we have  $\mathfrak{R}_0 = 12.6023 > 1$ . Based on Theorem 2, when  $\mathfrak{R}_0 > 1$  indicates that the disease will persists in the population. Figure 4 confirms the trajectory plot of (2) when  $\mathfrak{R}_0 > 1$ . All the population compartments converge to their endemic equilibrium.

From Figures 3 and 4, we can easily see that the rate of infected individuals perform medication  $\eta$  and the contact rate  $\beta$  have significant effect on the dynamics of TB population. Exposed, infected, and medicated subpopulations in TB dynamics experience a decrease in population numbers from the initial value until they reach a stable condition at the equilibrium point. When we decrease the value of  $\eta$ , the number of exposed and infected individuals increase. This show that the administration of medication has negative influence on the spread of the TB disease. While we increase the value of  $\beta$ , the number of exposed and infected individuals increase. This show that the contact rate has positive influence on the spread of the TB disease.

Figure 2. The relationship graph among  $R_0$ ,  $\beta$ , and  $\eta$ Figure 3. The trajectory plot of the (2) when  $R_0 < 1$ Figure 4. The trajectory plot of the (2) when  $R_0 > 1$ 

#### 4. CONCLUSION

This study analyzes tuberculosis (TB) dynamics using a compartmental SEIM model that divides the population into four classes: susceptible, exposed, infected, and medicated. The mathematical analysis identifies two equilibrium points: endemic and non-endemic. The stability of these points is evaluated using Lyapunov functions, demonstrating global stability under specific conditions. The non-endemic equilibrium is globally stable when  $R_0 < 1$ , suggesting disease eradication, while the endemic equilibrium is stable when  $R_0 > 1$ , indicating persistent TB transmission. The numerical simulations and sensitivity analyses reveal that reducing the contact rate significantly decreases the spread of TB, while increasing the percentage of patients adhering to medication reduces transmission effectively. However, eradicating TB requires a multifaceted approach that goes beyond promoting medication adherence. Strategies must include reducing contact rates between vulnerable and infected individuals through targeted public health interventions.

From a public health perspective, this study underscores the importance of early detection and effective treatment strategies. Public health authorities should ensure timely contact investigations and adopt proactive measures to limit the spread of TB. Moreover, addressing challenges such as medication toxicity and ensuring adherence are critical for achieving sustained TB control. Future research should explore the integration of vaccination dynamics and resistance patterns to enhance the model's applicability in diverse epidemiological settings.

## FUNDING INFORMATION

This work is supported by the Non-State Revenue and Expenditure Budget Document for Budget Implementation Sources of Tuition Fees and Original Income of the Faculty of Science and Mathematics 2024 “NONAPBN DPA SUKPA FSM” (2024), Diponegoro University, Semarang, Indonesia, under contract number 25.II.F/UN7.F8/PP/II/2024

## AUTHOR CONTRIBUTIONS STATEMENT

This journal uses the Contributor Roles Taxonomy (CRediT) to recognize individual author contributions, reduce authorship disputes, and facilitate collaboration. The contributions of the authors to this study are detailed as follows:

Name of Author	C	M	So	Va	Fo	I	R	D	O	E	Vi	Su	P	Fu
Jovian Dian Pratama	✓		✓		✓			✓	✓	✓	✓		✓	
Anindya Henindya Permatasari	✓	✓	✓	✓		✓	✓	✓	✓		✓	✓	✓	✓

C : **C**onceptualization

M : **M**ethodology

So : **S**oftware

Va : **V**alidation

Fo : **F**ormal analysis

I : **I**nvestigation

R : **R**esources

D : **D**ata Curation

O : Writing - **O**riginal Draft

E : Writing - Review & **E**diting

Vi : **V**isualization

Su : **S**upervision

P : **P**roject administration

Fu : **F**unding acquisition

## CONFLICT OF INTEREST STATEMENT

The authors declare that they have no known competing financial interests or personal relationships that could have appeared to influence the work reported in this paper.

## ETHICAL APPROVAL

This study did not involve human participants or animals and is based entirely on computational modeling and theoretical analysis. Therefore, ethical approval was not required. The research was conducted in accordance with relevant institutional and international guidelines and standards for scientific integrity and responsible research conduct.

## DATA AVAILABILITY

This study utilized computational simulation data to model two conditions based on the basic reproduction number ( $\mathfrak{R}_0 < 1$  and  $\mathfrak{R}_0 > 1$ ). No real-world or empirical data were used. The simulation data and results can be fully reproduced using the methodology and parameters described in the article. The simulations were performed using Maple and MATLAB software. All relevant simulation data are included within the article and/or its supplementary materials. Additionally, the data are available from the corresponding author, [AHP], upon reasonable request.

## REFERENCES




- [1] R. Gopalaswamy, V. N. A. Dusthacker, S. Kannayan, and S. Subbian, “Extrapulmonary tuberculosis—an update on the diagnosis, treatment and drug resistance,” *Journal of Respiration*, vol. 1, no. 2, pp. 141–164, May 2021, doi: 10.3390/jor1020015.
- [2] J. W. Uzorka *et al.*, “Abnormalities suggestive of latent tuberculosis infection on chest radiography; how specific are they?,” *Journal of Clinical Tuberculosis and Other Mycobacterial Diseases*, vol. 15, p. 100089, May 2019, doi: 10.1016/j.jctube.2019.01.004.
- [3] P. Haldar, “The natural history of TB and latent infection,” in *Tuberculosis in Clinical Practice*, Cham: Springer International Publishing, 2021, pp. 1–14. doi: 10.1007/978-3-030-75509-6\_1.
- [4] S. Lee, L. Lau, K. Lim, J. Ferma, W. Dodd, and D. Cole, “The presence of cough and tuberculosis: active case finding outcomes in the philippines,” *Tuberculosis Research and Treatment*, vol. 2019, pp. 1–9, Aug. 2019, doi: 10.1155/2019/4578329.
- [5] World Health Organization, “Systematic screening for active tuberculosis: Principles and recommendations,” 2015. [Online]. Available: [https://www.who.int/tb/screening/en/%0Ahttp://apps.who.int/iris/bitstream/10665/84971/1/9789241548601\\_eng.pdf?ua=1](https://www.who.int/tb/screening/en/%0Ahttp://apps.who.int/iris/bitstream/10665/84971/1/9789241548601_eng.pdf?ua=1) (accessed: Dec 11, 2023).
- [6] A. S. Bohlbro, V. S. Hvingelby, F. Rudolf, C. Wejse, and C. B. Patsche, “Active case-finding of tuberculosis in general populations and at-risk groups: a systematic review and meta-analysis,” *European Respiratory Journal*, vol. 58, no. 4, p. 2100090, Oct. 2021, doi: 10.1183/13993003.00090-2021.

- [7] Y. Chen *et al.*, "Epidemiological features and temporal trends of HIV-negative tuberculosis burden from 1990 to 2019: a retrospective analysis based on the Global Burden of Disease Study 2019," *BMJ Open*, vol. 13, no. 9, p. e074134, Sep. 2023, doi: 10.1136/bmjopen-2023-074134.
- [8] World Health Organization (WHO), "Global tuberculosis report 2023," 2023. [Online]. Available: <https://www.who.int/publications/i/item/9789240083851> (accessed: Sep 11, 2023).
- [9] N. F. Khabibullina, D. M. Kutuzova, I. A. Burmistrova, and I. V. Lyadova, "The biological and clinical aspects of a latent tuberculosis infection," *Tropical Medicine and Infectious Disease*, vol. 7, no. 3, p. 48, Mar. 2022, doi: 10.3390/tropicalmed7030048.
- [10] A. S. Chitnis, D. Jaganath, R. G. Gish, and R. J. Wong, "Diagnosis and treatment of latent tuberculosis infection," *American Journal of Gastroenterology*, vol. 116, no. 11, pp. 2155–2158, Nov. 2021, doi: 10.14309/ajg.0000000000001398.
- [11] N. F. Khabibullina, D. M. Kutuzova, I. A. Burmistrova, and I. V. Lyadova, "The biological and clinical aspects of a latent tuberculosis infection," *Tropical Medicine and Infectious Disease*, vol. 7, no. 3, p. 48, Mar. 2022, doi: 10.3390/tropicalmed7030048.
- [12] L. Mastorino *et al.*, "Risk of reactivation of latent tuberculosis in psoriasis patients on biologic therapies: A retrospective cohort from a tertiary care centre in Northern Italy," *Acta Dermato-Venereologica*, vol. 102, p. adv00821, Nov. 2022, doi: 10.2340/actadv.v102.1982.
- [13] S. E. Dorman *et al.*, "Four-month rifapentine regimens with or without moxifloxacin for tuberculosis," *New England Journal of Medicine*, vol. 384, no. 18, pp. 1705–1718, May 2021, doi: 10.1056/NEJMoa2033400.
- [14] T. N. Jilani, A. Avula, A. Zafar Gondal, and A. H. Siddiqui, "Active tuberculosis," Treasure Island (FL), 2025.
- [15] M. Badrinath, R. J. Chen, and S. John, "Isoniazid toxicity," in *StatPearls*, 2024.
- [16] A. Thapa *et al.*, "Case Report: Acute isoniazid intoxication after intentional ingestion," *Wellcome Open Research*, vol. 7, p. 219, Aug. 2022, doi: 10.12688/wellcomeopenres.18068.1.
- [17] Q. Li and F. Wang, "An epidemiological model for tuberculosis considering environmental transmission and reinfection," *Mathematics*, vol. 11, no. 11, p. 2423, May 2023, doi: 10.3390/math11112423.
- [18] M. M. Ojo, O. J. Peter, E. F. D. Goufo, H. S. Panigoro, and F. A. Oguntolu, "Mathematical model for control of tuberculosis epidemiology," *Journal of Applied Mathematics and Computing*, vol. 69, no. 1, pp. 69–87, Feb. 2023, doi: 10.1007/s12190-022-01734-x.
- [19] I. Ullah, S. Ahmad, Q. Al-Mdallal, Z. A. Khan, H. Khan, and A. Khan, "Stability analysis of a dynamical model of tuberculosis with incomplete treatment," *Advances in Difference Equations*, vol. 2020, no. 1, p. 499, Dec. 2020, doi: 10.1186/s13662-020-02950-0.
- [20] S. Side, U. Mulbar, S. Sidjara, and W. Sanusi, "A SEIR model for transmission of tuberculosis," in *AIP Conference Proceedings*, 2017, doi: 10.1063/1.4980867.
- [21] K. Das, B. S. N. Murthy, S. A. Samad, and M. H. A. Biswas, "Mathematical transmission analysis of SEIR tuberculosis disease model," *Sensors International*, vol. 2, 2021, doi: 10.1016/j.sintl.2021.100120.
- [22] S. L. Chasanah, D. Aldila, and H. Tasman, "Mathematical analysis of a tuberculosis transmission model with vaccination in an age structured population," 2019, p. 020018, doi: 10.1063/1.5094282.
- [23] Fatmawati, M. Altaf Khan, E. Bonyah, Z. Hammouch, and E. Mifta Shaiful, "A mathematical model of tuberculosis (TB) transmission with children and adults groups: A fractional model," *AIMS Mathematics*, vol. 5, no. 4, pp. 2813–2842, 2020, doi: 10.3934/math.2020181.
- [24] D. Aldila, Z. A. Sari Ryanto, and A. Bustamam, "A mathematical model of TB control with vaccination in an age-structured susceptible population," *Journal of Physics: Conference Series*, vol. 1108, p. 012050, Nov. 2018, doi: 10.1088/1742-6596/1108/1/012050.
- [25] S. L. Chasanah, D. Aldila, and H. Tasman, "Mathematical analysis of a tuberculosis transmission model with vaccination in an age structured population," in *AIP Conference Proceedings*, 2019, p. 020018, doi: 10.1063/1.5094282.
- [26] H. M. Dewi, Widowati, R. Herdiana, and P. S. Sasongko, "Stability analysis of coronavirus disease spread model in Central Java province, Indonesia," in *AIP Conference Proceedings*, 2023, p. 080014, doi: 10.1063/5.0105905.
- [27] S. M. Rahmasari, Widowati, and R. Herdiana, "Mathematical modelling and stability analysis of the SEQIRD model spread of COVID-19," in *AIP Conference Proceedings*, 2023, p. 020015, doi: 10.1063/5.0140163.
- [28] O. Diekmann, M. Gyllenberg, and J. A. J. Metz, "Finite dimensional state representation of physiologically structured populations," *Journal of Mathematical Biology*, vol. 80, no. 1–2, pp. 205–273, Jan. 2020, doi: 10.1007/s00285-019-01454-0.
- [29] B. Boldin, O. Diekmann, and J. A. J. Metz, "Population growth in discrete time: a renewal equation oriented survey," *Journal of Difference Equations and Applications*, vol. 30, no. 8, pp. 1062–1090, Aug. 2024, doi: 10.1080/10236198.2023.2265499.
- [30] S. M. Lalaoui Ben Cherif, O. Balatif, and O. Kebiri, "Analysis and optimal control of a vaccinated pandemic covid-19 model," *Journal of Mathematical Sciences*, vol. 280, no. 4, pp. 582–604, Apr. 2024, doi: 10.1007/s10958-024-06992-7.
- [31] D. Y. Trejos, J. C. Valverde, and E. Venturino, "Dynamics of infectious diseases: A review of the main biological aspects and their mathematical translation," *Applied Mathematics and Nonlinear Sciences*, vol. 7, no. 1, pp. 1–26, Jan. 2022, doi: 10.2478/amns.2021.1.00012.
- [32] A. Savadogo, B. Sangaré, and H. Ouedraogo, "A mathematical analysis of Hopf-bifurcation in a prey-predator model with nonlinear functional response," *Advances in Difference Equations*, vol. 2021, no. 1, p. 275, Dec. 2021, doi: 10.1186/s13662-021-03437-2.
- [33] M. A. Aziz-Alaoui, J. M.-S. Lubuma, and B. Tsanou, "Prevalence-based modeling approach of schistosomiasis: global stability analysis and integrated control assessment," *Computational and Applied Mathematics*, vol. 40, no. 1, p. 24, Feb. 2021, doi: 10.1007/s40314-021-01414-9.
- [34] X. Fu, M. Huang, C. K. Tse, J. Yang, Y. Ling, and X. Zha, "Synchronization stability of grid-following VSC considering interactions of inner current loop and parallel-connected converters," *IEEE Transactions on Smart Grid*, vol. 14, no. 6, pp. 4230–4241, Nov. 2023, doi: 10.1109/TSG.2023.3262756.
- [35] X. Fu *et al.*, "Large-signal stability of grid-forming and grid-following controls in voltage source converter: a comparative study," *IEEE Transactions on Power Electronics*, vol. 36, no. 7, pp. 7832–7840, Jul. 2021, doi: 10.1109/TPEL.2020.3047480.
- [36] N. V. Kuznetsov, T. N. Mokaev, A. A.-H. Shoreh, A. Prasad, and M. D. Shirmali, "Analytical and numerical study of the hidden boundary of practical stability: complex versus real Lorenz systems," *arXiv*, 2021.
- [37] H. Gulbudak, Z. Qu, F. Milner, and N. Tuncer, "Sensitivity analysis in an immuno-epidemiological vector-host model," *Bulletin of Mathematical Biology*, vol. 84, no. 2, p. 27, Feb. 2022, doi: 10.1007/s11538-021-00979-0.
- [38] Y. M. Rangkuti, Firmansyah, and A. Landong, "Sensitivity analysis of SEIR epidemic model of Covid 19 spread in Indonesia," *Journal of Physics: Conference Series*, vol. 2193, no. 1, p. 012092, Feb. 2022, doi: 10.1088/1742-6596/2193/1/012092.
- [39] K. M. Gostic *et al.*, "Practical considerations for measuring the effective reproductive number,  $R_t$ ," Jun. 21, 2020, doi: 10.1101/2020.06.18.20134858.
- [40] M. C. Nunes *et al.*, "Redefining pandemic preparedness: Multidisciplinary insights from the CERP modelling workshop in infectious diseases, workshop report," *Infectious Disease Modelling*, vol. 9, no. 2, pp. 501–518, Jun. 2024, doi: 10.1016/j.idm.2024.02.008.




- [41] A. G. Buchwald, J. Adams, D. M. Bortz, and E. J. Carlton, "Infectious disease transmission models to predict, evaluate, and improve understanding of covid-19 trajectory and interventions," *Annals of the American Thoracic Society*, vol. 17, no. 10, pp. 1204–1206, Oct. 2020, doi: 10.1513/AnnalsATS.202005-501PS.
- [42] A. P. Zhao *et al.*, "AI for science: Predicting infectious diseases," *Journal of Safety Science and Resilience*, vol. 5, no. 2, pp. 130–146, Jun. 2024, doi: 10.1016/j.jnlssr.2024.02.002.

## BIOGRAPHIES OF AUTHORS



**Jovian Dian Pratama**    was born in Semarang on August 28, 1997. He graduated with honors (Cum Laude) from the Undergraduate Program in Mathematics at the Faculty of Science and Mathematics, Diponegoro University (UNDIP) in 2020. He completed his master's degree with Cum Laude distinction, a perfect GPA, and he was the Best Graduate in the master's Program in Mathematics at the Faculty of Science and Mathematics, Diponegoro University (UNDIP) in 2022. Jovian has been a full-time lecturer in the Department of Mathematics, Faculty of Science and Mathematics, Diponegoro University, Semarang, since 2022. His area of expertise is applied mathematics, with a particular focus on applied numerical analysis and computation. He can be contacted at email: joviandianp@lecturer.undip.ac.id or joviandianpratama@yahoo.com.



**Anindita Henindya Permatasari**    was born in Semarang, May 23, 1993. Graduated with a bachelor's degree in mathematics from Diponegoro University in 2015. Graduated with a master's degree in mathematics from Diponegoro University in 2018. Since 2019, she has been accepted as a permanent lecturer at the Department of Mathematics, Faculty of Science and Mathematics, Diponegoro University, Semarang. She is a member of the Applied Mathematics Expertise Group, which focuses on studies on the application of mathematics in the fields of science and technology, social and industry. She focuses on research themes such as infectious disease modeling, dynamic systems and optimal control, and stochastic modeling. She can be contacted at email: aninditahenindya@lecturer.undip.ac.id.